COLLEGE OF ENGINEERING
NUCLEAR ENGINEERING & RADIOLOGICAL SCIENCES
UNIVERSITY OF MICHIGAN

Nuclear Reactor
Analysis & Methods
Group
NuRAM

NE/8887/2020-002-00
NURAM-2020-003-00

Assessment of Variable Reflector Reactivity Envelope in Multi-Module HTGR Special Purpose Reactor

Brendan Kochunas, Kaitlyn Barr, and Shai Kinast

University of Michigan

07/31/2020

NEUP Nuclear Energy University Program
U.S. Department of Energy

This page is intentionally blank.

REVISION LOG

Revision	Date	Affected Pages	Revision Description
0	07/31/2020	All	Initial Release

Document pages that are:

Export Controlled:	None
IP/Proprietary/NDA Controlled:	None
Sensitive Controlled:	None
Unlimited:	All

This work was supported by funding received from the DOE Office of Nuclear Energy's Nuclear Energy University Program under contract number DE-NE0008887.

COLLEGE OF ENGINEERING
NUCLEAR ENGINEERING & RADIOLOGICAL SCIENCES
UNIVERSITY OF MICHIGAN

Argonne NATIONAL LABORATORY

HolosGen™

EXECUTIVE SUMMARY

In this report we examine the reactivity that is available in the reflectors (i.e. the reactivity envelope) through several mechanisms that may be understood notionally as a "variable reflector". Specifically we assess in detail the reactivity of:

- Subcritical Power Module (SPM)
- Control Drum Rotation Patterns
- Moderating power of the outer radial reflector
- Moderating power of the central cross reflector

for the Holos-Quad microreactor design.

All mechanisms demonstrate quantitatively a sufficient range of reactivity that control is possible for load follow operation. The reactivity due to the SPM position is quite large at **220 pcm/cm** in position. As a result this mechanism is not ideal for control for Flexible Power Operation (FPO). Moreover, the Holos-Quad design as undergone further development, and positioning of the SPM is no longer a feature of the design.

The reactivity of the control drums is quite flexible by varying the pattern in which the drums are rotated. Depending on the number of drums rotated the reactivity worth can be anywhere from **1 up to 400 pcm per degree rotation**. This is determined to be a suitable control mechanism for FPO. Furthermore, analytic models for the integral drum reactivity worth and differential drum reactivity are derived based on first order perturbation theory and shown to suitable for representing the reactivity worth curves determined from detailed Monte Carlo calculations. The development of the analytical models will be an important tool for future work on the design and assessment of control algorithms for FPO.

The moderating power of the reflectors, either central or radial, is examined for 10% to 200% nominal density–while there is not a physical mechanism or ability to create these materials it neverthless provides important information as to the reactivity as parameterized by the reflector effective total cross section and scattering ratio. From this assessment we observe that the outer reflector worth is about $\sim$**44pcm per** $\Delta V\%V$ and $\sim$**22pcm per** $\Delta V\%V$. These values also suggest this as a mechanism suitable for reactivity control enabling FPO. However, we have not yet determined a passive mechanism through which these changes might be achieved. One option would be to develop a stratified radial reflector with plates of reflector material where the spacing in between can be adjusted using changes in temperature of gas or thermal expansion of another material. Alternatively, mechanisms to rotate the drums that operate passively may also be feasible.

CONTENTS

LIST OF FIGURES

LIST OF TABLES

ACRONYMS

ANL Argonne National Laboratory

FPO Flexible Power Operation

HTGR High Temperature Gas Reactor

QOI Quantity of Interest

SAM Systems Analysis Module

SPM Subcritical Power Module

TH Thermal Hydraulics/Fluids

1. INTRODUCTION

1.1 Scope and Objectives

The overall aim of this project is to investigate and develop passive systems for autonomous control of High Temperature Gas Reactor (HTGR) special purpose reactors–or microreactors. In previous work [1], we investigated the reactivity of local temperature perturbations as one mode of physics for passive control. In this report we investigate the feasibility of passive control by characterizing the leakage reactivity and corresponding parameter space of the reflector cross sections.

The specific objective is to identify the full range of reactivity perturbations achievable (e.g. the reactivity envelope) through modification of the reflector physics of the microreactor. For microreactors we assume, due to their small size, that the reactivity envelope of the reflector due to leakage is much greater than that due to local temperature changes and doppler feedback. The notion of the variable reflector is explored by several approaches:

1. the spacing between the SPM,
2. the rotational position of various combinations of control drums,
3. the total cross section of the radial reflector (via a change in density),
4. the total cross section of the central cross reflector (again via changing density).

1.2 Background

As a specific use case for an HTGR we use the reactor design under development at Holos. The Holos-Quad design is a scaled down HTGR with the core being composed of four SPMs. Each SPM is effectively an independent closed loop Brayton cycle power conversion unit with a nuclear heat source in a tube-shell heat exchanger configuration. This effectively eliminates the balance of plant. When the four SPMs are configured properly they will create a critical reactor. An illustration of the SPM is shown in A publicly available preliminary neutronic design of this reactor

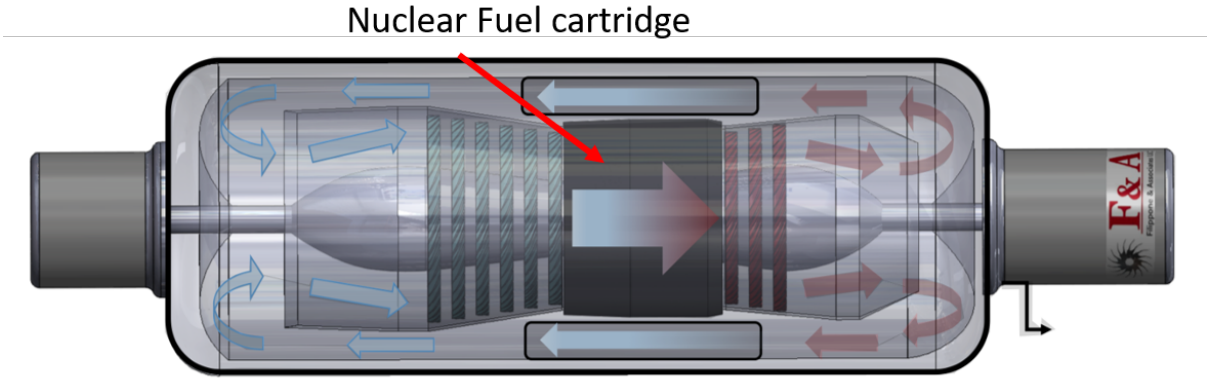

Figure 1. Illustration of an SPM

is described in [2]. This design was used as the basis for our previous work [1]. A key feature of the Holos-Quad was was its separable SPMs. The public design is illustrated in Fig. 2a with all SPMs inserted, and with SPMs separated in Fig. 2b.

However, since that time, the design has continued to evolve under the ARPA-E MEITNER program [3]. This new, proprietary design was developed by the ARPA-E Resource team at Argonne National Laboratory (ANL) and finalized on April 20th, 2020 [4]. The updated core design analyzed in this report refers to a configuration wherein the SPMs are still physically separated, but fixed in their quadrant, the SPMs are no longer actuated or moved to change reactivity. Additionally, there exists a central cruciform reflector between the SPMs. The final design still uses 8 control drums. The control drums from the preliminary design are shown in Section 1.2 with all drums in and out. This new proprietary design serves as the primary basis for the calculations and assessments performed and documented in this report. However, the design given in [2] is still used to characterize the reactivity of the SPM spacing.

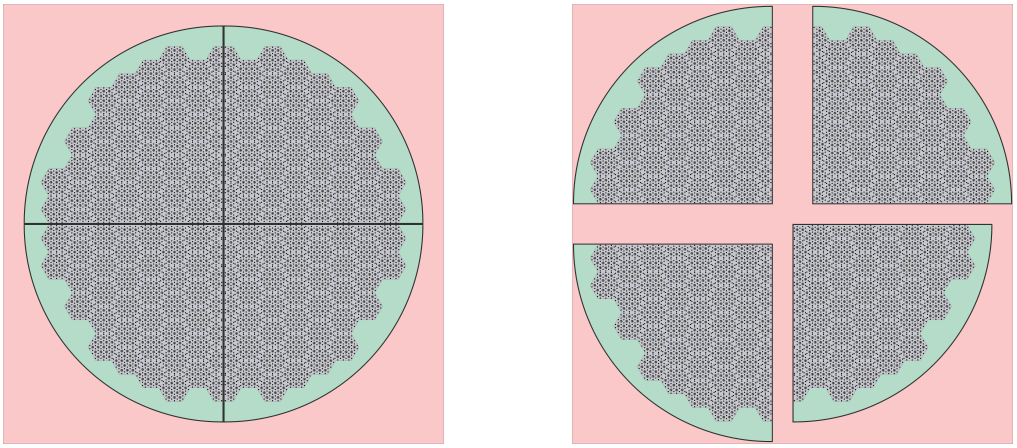

(a) Holos-Quad with SPMs together **(b) Holos-Quad with SPMs apart**

Figure 2. Preliminary Holos-Quad Design

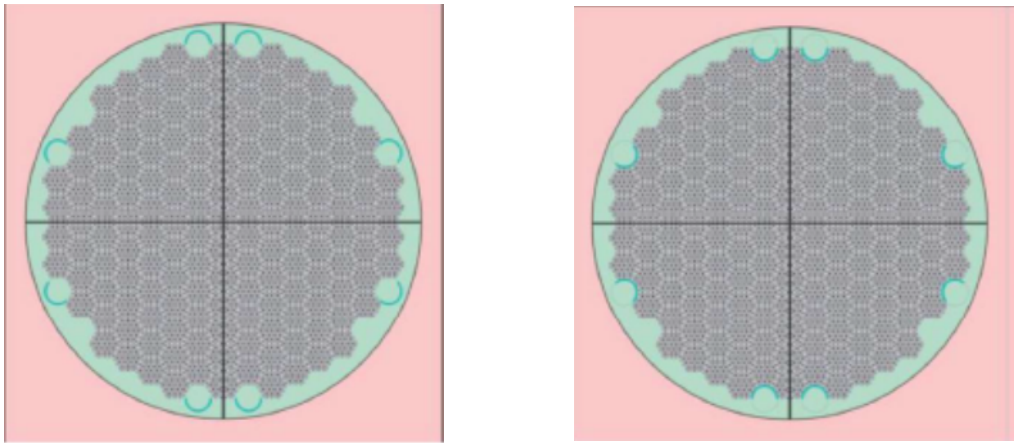

(a) Holos-Quad with Drums Out **(b) Holos-Quad with Drums In**

Figure 3. Preliminary Holos-Quad Control Drum Design

2. METHODOLOGY

The primary approach to characterize the reflector reactivity was to use run a multitude of Monte Carlo neutron transport calculations. Some of the details of these calculations are provided in the following subsection.

In addition to the numerical calculations, we utilized first order perturbation theory to derive approximate analytical expressions for the reactivity with some intuition. As will be seen in Section 3 this is capable of providing highly accurate results in some cases, and it is likely that further generalization is possible to further improve accuracy.

2.1 Monte Carlo Calculations

Numerical calculations of the reactivity of the reactor were performed at various conditions using the Monte Carlo code Serpent [5]. The calculations used ENDF-B7.1 nuclear data with materials at operating conditions. The extent of the core model included explicit treatment of all core structures and components out to the ISO container boundary. The operating temperature profiles included 10 axial segments and 18 unique radial temperature zones in each level. The assigned temperatures came from calculations by the Systems Analysis Module (SAM) code and essentially followed the same approach as documented in [1]. The majority of the simulations were run with 100 inactive cycles, 500 total cycles, and 10,000 particles per cycle to reduce run times. This resulted in uncertainties of 40 pcm to 60 pcm in k_{eff} . Some cases used more particles for reduced uncertainties.

The base models were provided by ANL and modified to allow each control drum to be positioned independently in 10° increments. These models were used to calculated integral and differential control drum worth curves for 12 different drum patterns.

Additionally, these models were used to artificially adjust the density of the central and outer radial reflector materials. The densities were adjusted with a multiplier ranging from 10% to 200% nominal density in 10% increments.

Due to the proprietary nature of the reactor design, no further details of the models are given. However, detailed geometric, material, and other design parameters can be provided with a direct request to HolosGen.

2.1.1 Uncertainty Propagation for Reactivity

The results reported in Section 3 include proper uncertainty propagation of k_{eff} to the reactivity ρ. The equation for the reactivity, ρ is

$$\rho = \frac{1}{k_{\text{ref}}} - \frac{1}{k_{\text{perturb}}}, \tag{1}$$

where k_{ref} is the multiplication factor for the reference condition (e.g. drums out) and k_{perturb} is the multiplication factor of the perturbed state (e.g. drums in). We desire to have the associated uncertainty of σ_ρ given the uncertainties of k_{ref} and k_{perturb}, denoted σ_{ref} and σ_{perturb}, respectively.

The fundamental formulas for the uncertainty propagation for basic arithmetic operations involved

are given as:

$$\sigma_{\pm} = \sqrt{a^2\sigma_X^2 + b^2\sigma_Y^2 \pm 2ab\sigma_{XY}}, \tag{2a}$$

$$\sigma_{\times \text{ or } \div} = |f(X,Y)|\sqrt{\left(\frac{\sigma_X}{X}\right)^2 + \left(\frac{\sigma_Y}{Y}\right)^2 \pm 2\frac{\sigma_{XY}}{XY}}. \tag{2b}$$

where X and Y have standard deviations σ_X and σ_Y, respectively, and covariance σ_{XY}. The symbols a and b are constants. The function $f(X,Y)$ is either XY or X/Y. Assuming no covariances, and through some algebra, the statistical uncertainty of the reactivity is obtained as

$$\sigma_\rho = |\rho|\sqrt{\frac{\sigma_{\text{perturb}}^2 + \sigma_{\text{ref}}^2}{\left(k_{\text{perturb}} - k_{\text{ref}}\right)^2} + \left(\frac{\sigma_{\text{perturb}}}{k_{\text{perturb}}}\right)^2 + \left(\frac{\sigma_{\text{ref}}}{k_{\text{ref}}}\right)^2}. \tag{3}$$

Equation (3) is the formula used to obtain the error bars on the reactivity plots in Section 3.

2.2 First Order Perturbation Theory

2.2.1 Background

First order perturbation theory has long been a useful tool in reactor physics. In this subsection we briefly review some of the fundamental equations and associated assumptions to arrive at simple expressions for the reactivity. The resulting equations will then be used to develop simplified analytical expressions for the control drum reactivity worth curves.

We begin with the equation for reactivity using first order perturbation theory. The derivation of which is readily found in nuclear engineering textbooks [6].

$$\rho = \frac{\delta k}{k} = \frac{\left\langle \phi^*, \left(\frac{1}{k}\boldsymbol{\delta F} - \boldsymbol{\delta M}\right)\phi \right\rangle}{\frac{1}{k}\left\langle \phi^*, \boldsymbol{\delta F}\phi \right\rangle}, \tag{4}$$

here δk, $\boldsymbol{\delta F}$, and $\boldsymbol{\delta M}$ are the perturbations to the multiplication factor, fission operator, and migration and loss operator, respectively. The scalar flux is denoted by ϕ and its adjoint, ϕ^*. The fission operator, $\boldsymbol{F}$, and migration-loss operator, $\boldsymbol{M}$, simply satisfy the neutron balance equation and can generally represent transport or diffusion and multigroup or continuous energy forms. The main approximation of first order perturbation theory is to assume that the perturbed scalar flux is well represented by the unperturbed scalar flux in both space and energy. This is generally true for small perturbations. It follows naturally that perturbations to the reactor that do not induce strong spectral changes or changes to the shape of the scalar flux are well represented by first order perturbation theory.

We consider now the justification of this assumption to microreactors and insist that for perturbations to temperature that are global and uniform, or for perturbations to the radial reflector composition or leakage rate are likely to be well represented by first order perturbation theory. As we will see in Section 3 this is true in many, but not all, cases for perturbations to the reflector.

Next we wish to further simplify Eq. (4) by simplifying the operators $\boldsymbol{\delta F}$, and $\boldsymbol{\delta M}$. For these operators we assume one-speed diffusion so that they may be written explicitly as:

$$\boldsymbol{\delta M} = -\nabla \cdot \delta D \nabla + \delta\Sigma_a, \tag{5a}$$

$$\boldsymbol{\delta F} = \delta(\nu\Sigma_f), \tag{5b}$$

where δD, $\delta\Sigma_a$, and $\delta(\nu\Sigma_f)$ are the perturbations to the diffusion coefficient, absorption cross section, and fission production cross section, respectively. Substituting Eq. (5) into Eq. (4) yields:

$$\rho = \frac{\int_V \phi^* \left[\frac{1}{k}\delta\left(\nu\Sigma_f\right)\phi + \nabla\cdot\delta D\nabla\phi - \delta\Sigma_a\phi\right] dV}{\frac{1}{k}\int_V \nu\Sigma_f\phi^*\phi dV}. \tag{6}$$

Further, recalling that the one-speed diffusion equation is self-adjoint leads to:

$$\rho = \frac{\int_V \frac{1}{k}\delta\left(\nu\Sigma_f\right)\phi^2 + \nabla\cdot\delta D\nabla\phi^2 - \delta\Sigma_a\phi^2 dV}{\frac{1}{k}\int_V \nu\Sigma_f\phi^2 dV}. \tag{7}$$

The one-speed assumption is reasonable so long as accurate energy integrated effective cross sections (and their perturbations) can be obtained. Moreover, the conditions under which we make the assumptions regarding the accuracy of first order perturbation theory allow us to confidently assume one-speed. The one-speed assumption will break down if perturbations to the system cause non-trivial spectral or shape changes in the scalar flux. Since have assumed this to be the case for first order perturbation theory, it applies equally usefully to one-speed diffusion. Perturbations to the diffusion coefficient or leakage, may be invalidate the assumption of diffusion since this is already questionable at the system boundary. However, our goal is to apply this theory to derive analytical expressions for the control drum worth, which we may reasonably assume do not cause perturbations to the diffusion coefficient.

2.2.2 Approximate analytical expressions for control drum reactivity worth curves

From the equation for the reactivity based on one-speed diffusion and first order perturbation theory, we further simplify Eq. (7) for the case of control drum movement. Specifically, we observe that perturbations induced by rotation of the control drums:

- do not cause perturbations to the fission cross section ($\delta(\nu\Sigma_f) = 0$)
- cause much larger perturbations in the absorption cross section than the diffusion coefficient ($\delta D << \delta\Sigma_a$), therefore we may neglect the perturbation to the diffusion coefficient ($\delta D \approxeq 0$).

Applying these assumptions to Eq. (7) yields:

$$\rho = \frac{\int_V -\delta\Sigma_a\phi^2 dV}{\frac{1}{k}\int_V \nu\Sigma_f\phi^2 dV} \tag{8}$$

If we further assume that the fission cross section, and perturbation to the absorption are uniform, then the integrals of the scalar flux cancel and we obtain:

$$\rho = \frac{-\delta\Sigma_a}{\Sigma_a + DB^2}. \tag{9}$$

Note this equation has been further simplified by the one-speed diffusion expression for k.

The next task at hand is to now derive, or rather develop by inference, a more explicit expression for $\delta\Sigma_a$. Here we wish to note that the uniformity of these coefficients, is quite similar to assuming

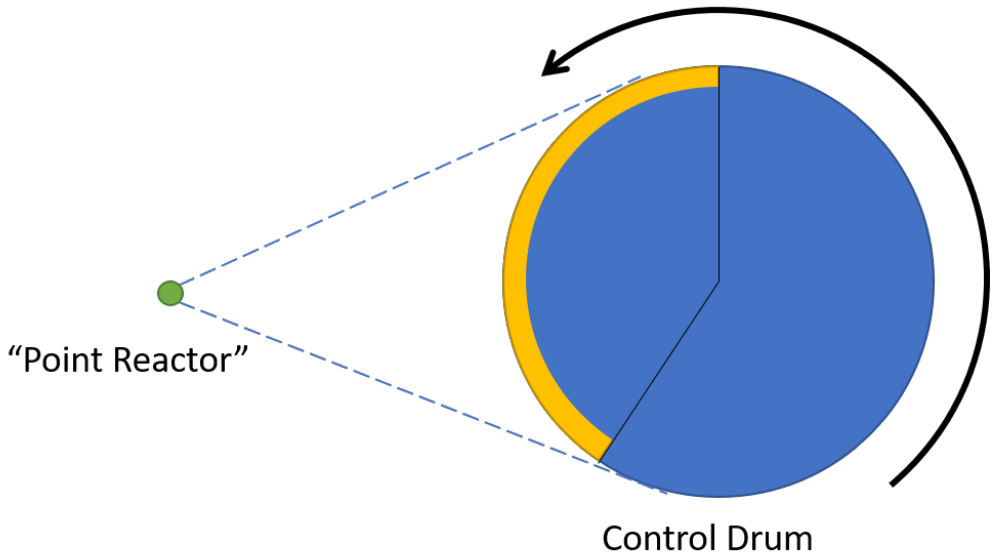

Figure 4. Point Reactor and Rotating Control Drum

a point reactor (although there are subtle differences). Conceiving of the problem as a point reactor and a control drum, we may conceptualize this problem in the way illustrated by Fig. 4.

Considering the "physics" of Fig. 4, we expect the absorption cross section (and reactivity–since it is proportional to $\delta\Sigma_a$) should vary in the following way, if the fully rotated in position is taken as the reference position (i.e. 0°).

- the maximum reactivity should occur at 180°
- the reactivity will increase when rotating from 0° to 180°
- rotating the drum further from 180° to 360° will cause the reactivity decrease
- the increase in reactivity from 0° to 180° should be symmetric to the decrease in reactivity from 180° to 360° .

Basic trigonometry informs us that the underlying function should be the sin or cos. An analogous problem to illustrate this would be the equation for the distance between a point next to a circle and a point on the edge of the circle as function of the rotational position of the circle.

The general form of the sine function can be expressed as:

$$f(\theta) = A \sin\left(\frac{\theta}{\lambda} + \omega\right) + K, \tag{10}$$

where A is the amplitude, K is the vertical shift, λ is the period, and ω is the phase shift. From our previous statements regarding the expectations of the reactivity (specifically it is the integral reactivity), the period, λ, should be 1. Since the minimum reactivity value should occur at 0° , and the maximum at 180° , this implies a phase shift of $-90°$ (or $+270°$). Because the sine function is bounded on the interval $[-1, 1]$, and from our above statements we desire the reactivity to exist on $[0, \rho_{\max}]$, this implies that $K = A$ and $A = \rho_{\max}/2$. We may now write explicitly, an equation for

the integral reactivity worth:

$$\boxed{\rho(\theta) = \frac{\rho_{\max}}{2}\left(1 - \cos\theta\right)}, \tag{11}$$

where $\rho_{\max}$ is:

$$\rho_{\max} = \frac{1}{k_{\text{drums out}}} - \frac{1}{k_{\text{drums in}}}. \tag{12}$$

Note that to obtain the form of Eq. (11) we have made use of the trigonometric identity $-\cos x = \sin x - \frac{\pi}{2}$. The differential control drum worth is readily obtained through differentiation of Eq. (11).

$$\boxed{\frac{d\rho(\theta)}{d\theta} = \frac{\rho_{\max}}{2}\sin\theta}, \tag{13}$$

3. RESULTS AND ANALYSIS

3.1 Control Drum Reactivity Assessment

The control drum integral and differential reactivity worth curves were assessed for 12 control drum patterns using drum rotation increments of 10° . The 12 drum patterns are shown in Fig. 5. These 12 patterns effectively cover each unique combination of drums as the even and odd drums have slightly different local geometries, and are not exactly equivalent. The patterns also include some that are highly asymmetric. The Monte Carlo and analytic integral and differential drum worth curves for each pattern are shown in Figs. 6 and 7, respectively.

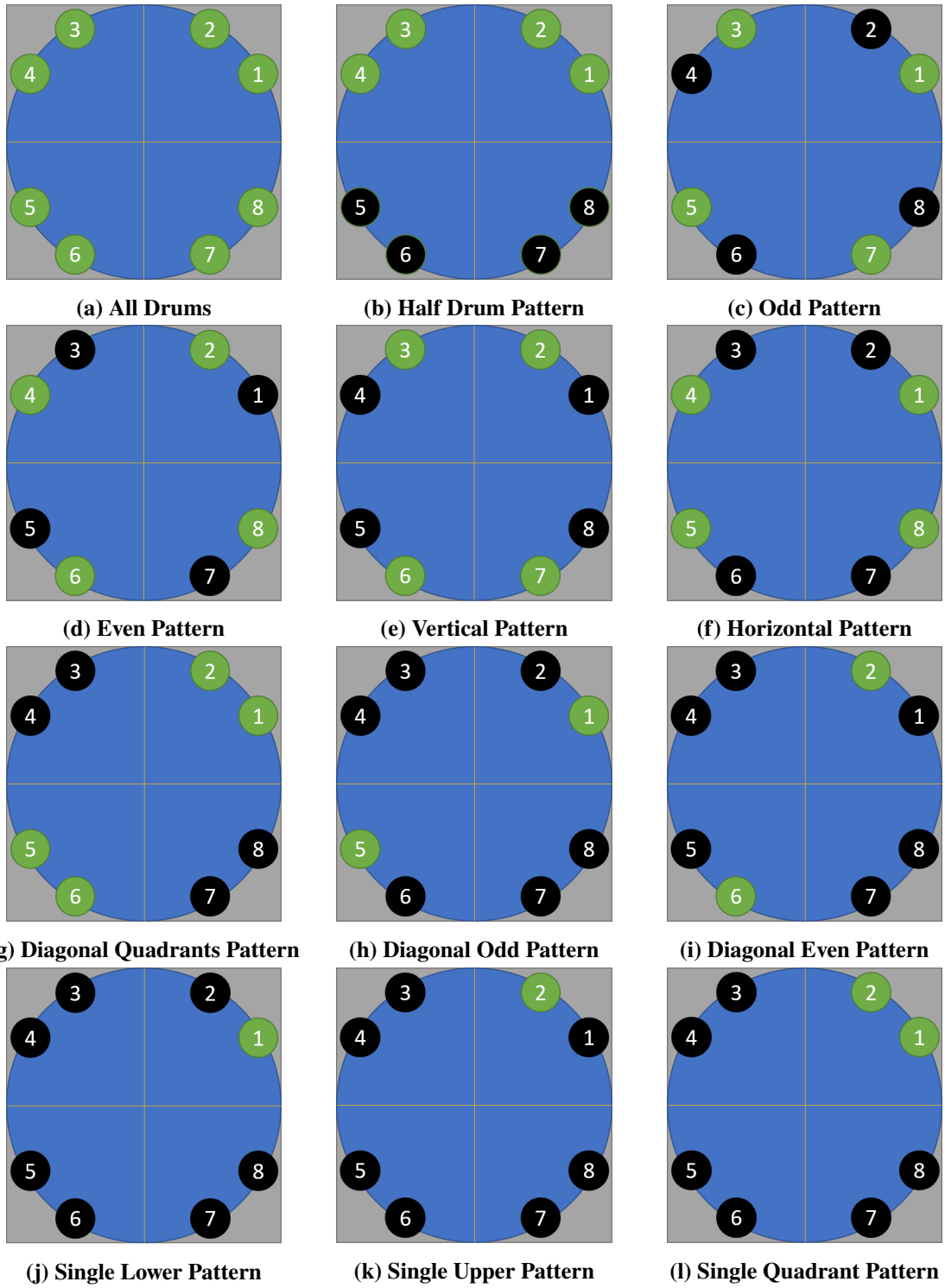

Figure 5. Control Drum Patterns (green indicates the drums that are rotated symmetrically for the given pattern; black are drums rotated out)

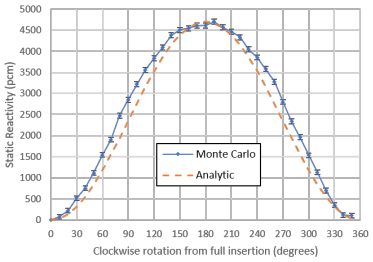

(a) All Drums

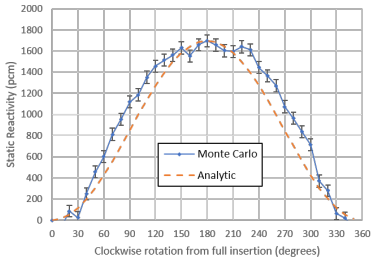

(b) Half Drum Pattern

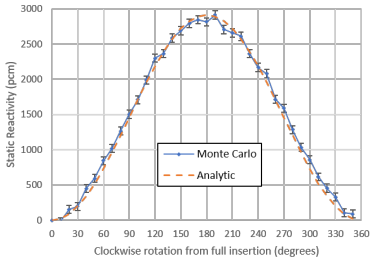

(c) Odd Pattern

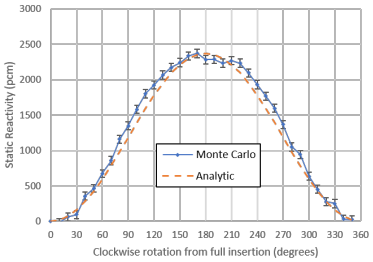

(d) Even Pattern

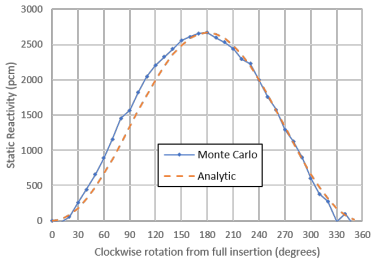

(e) Vertical Pattern

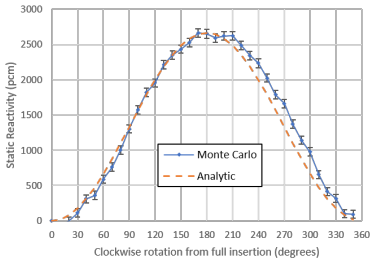

(f) Horizontal Pattern

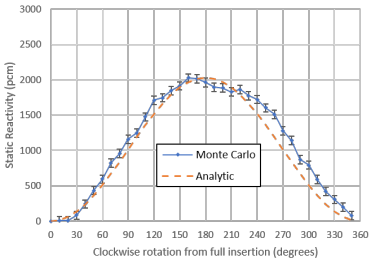

(g) Diagonal Quadrants Pattern

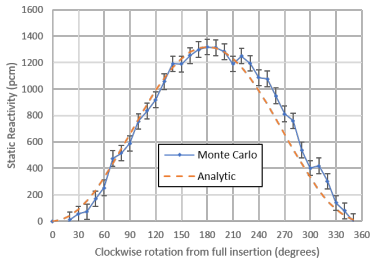

(h) Diagonal Odd Pattern

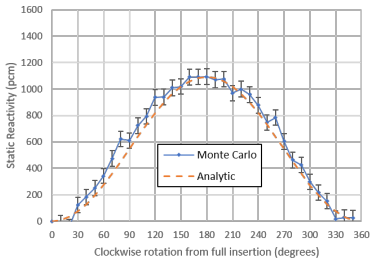

(i) Diagonal Even Pattern

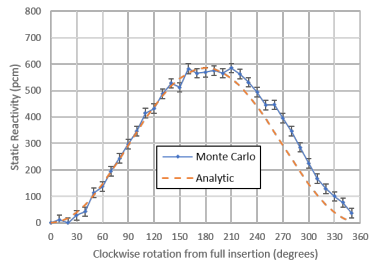

(j) Single Lower Pattern

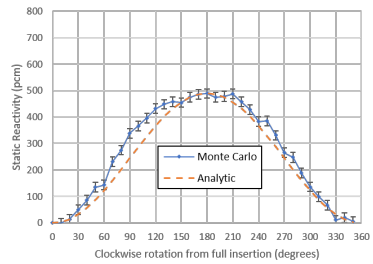

(k) Single Upper Pattern

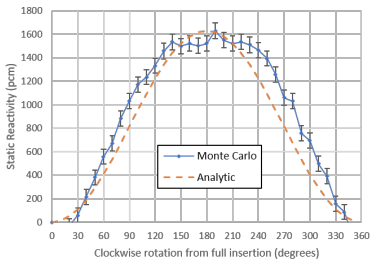

(l) Single Quadrant Pattern

Figure 6. Integral Control Drum Reactivity Worths

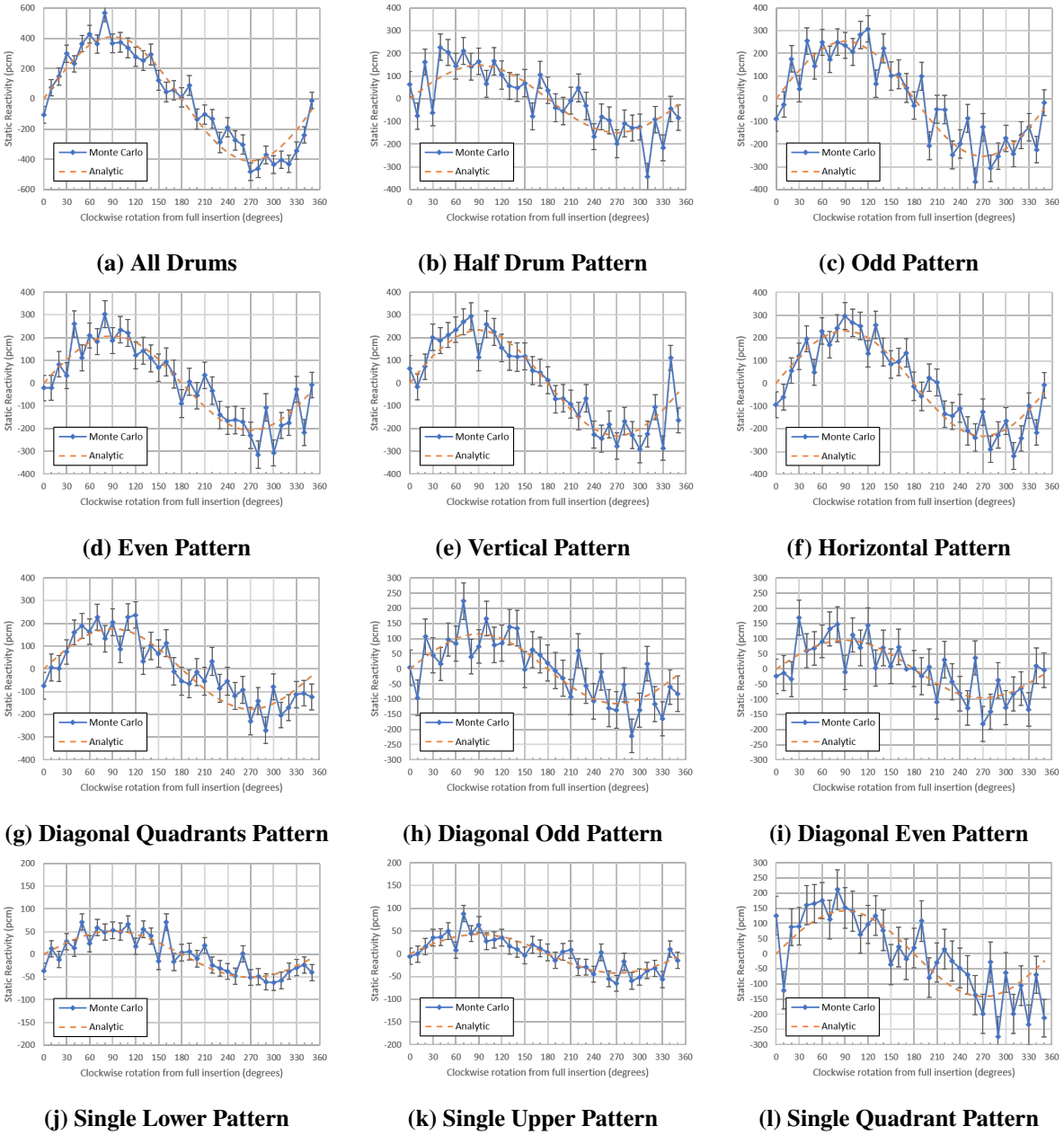

(a) All Drums (b) Half Drum Pattern (c) Odd Pattern

(d) Even Pattern (e) Vertical Pattern (f) Horizontal Pattern

(g) Diagonal Quadrants Pattern (h) Diagonal Odd Pattern (i) Diagonal Even Pattern

(j) Single Lower Pattern (k) Single Upper Pattern (l) Single Quadrant Pattern

Figure 7. Differential Control Drum Reactivity Worths

Several observations are made from the examination of Fig. 6. In all cases the integral drum worth curve is generally shaped in the form of Eq. (11). However, there are clear and systematic deviations for some cases. As a quantitative measure of the accuracy of the analytical model, $\rho(\theta_i)$, to Monte Carlo result, $\rho_{\mathrm{MC,i}}$, we use the following root mean square difference in reactivity.

$$\mathrm{RMS} = \sqrt{\frac{1}{N}\sum_{i}^{N}\left(\rho(\theta_i) - \rho_{\mathrm{MC,i}}\right)^2} \tag{14}$$

We compare this to an RMS of the Monte Carlo uncertainty,

$$\sigma_{\mathrm{RMS}} = \sqrt{\frac{1}{N}\sum_{i}^{N}\sigma_{\rho,i}^2} \tag{15}$$

and suggest that if the ratio is less 2, then "on average" Eq. (11) is predicting a reactivity worth within 2σ of the Monte Carlo uncertainty. A summary of the ratios for each case are provided in Table 1. Here we see that model provides a good prediction for 4 out of the 12 cases, and all but

Table 1. Comparison of Integral Drum Worths for Analytic Prediction and Monte Carlo Result by Relative RMS Measure Against Statistical Uncertainty

Case	$\mathrm{RMS}/\sigma_{\mathrm{RMS}}$
All	4.99
Half	2.90
Odd	1.32
Even	1.96
Vertical	2.30
Horizontal	2.42
Diagonal Quadrants	2.58
Diagonal Odd	1.56
Diagonal Even	1.08
Single Lower	2.65
Single Upper	2.18
Single Quadrant	2.63

one of the cases, the all drums in case, have a ratio between 2 and 3. It should not be surprising that the all drums case has the worst agreement to the model, since the model is, generally speaking, less valid for large perturbations, and this is the largest perturbation examined. The case with the best agreement is the diagonally symmetric rotation of the even numbered drums. We suggest that the good agreement observed for this case is due to cancellation of errors in Eq. (11) due to the symmetry of the problem. When the model provides a poorer prediction we attribute this to one or more of the assumptions that went into the model to be invalidated. Turning our attention closely to the "Single Upper" and "Single Lower" patterns we observe that the integral reactivity is not perfectly symmetric about the fully inserted position. This "feature" of integral drum worth asymmetry is generally observed in all the other cases exhibiting a poor prediction, and we attribute

this to slight asymmetries in the local geometry near the control drum. Because this deviation is systematic it suggests Eq. (11) may be modified to account for this. By inspection we observe that a simple way that we might account for this asymmetry is to add additional higher frequency terms (e.g. $\cos(2x)$ and $\sin(2x)$ to Eqs. (11) and (13), respectively) with some coefficients to be determined. Further augmentation or enhancement of Eqs. (11) and (13) will be a study of future work.

The differential drum worths follow inherently from the from the same data, and thus similar conclusions from this data may be drawn. We suggest then that the differential drum worths are merely a different way of viewing the same data. One note about viewing the differential drum worths is that the statistical uncertainty is relatively greater–due to the differential worth being smaller. In future work we will rerun these cases with more particles to refine the statistics.

The last point of analysis is to note that different whole core symmetric drum patterns involving differing numbers of drums provide scaled worth curves. This is illustrated by Fig. 8. This aspect of the reactor design provides a nice "menu" of drum patterns from which to control the reactor under various conditions, and its likely this can be used advantageously in a multiple input, multiple output control strategy to maximize operational life, optimize xenon oscillations, or optimize margin to Thermal Hydraulics/Fluids (TH) limits.

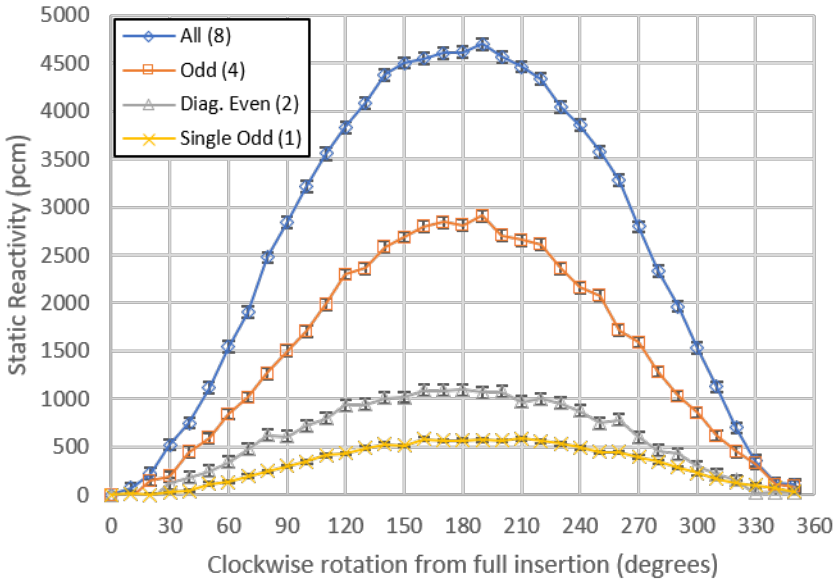

Figure 8. Comparisons of Integral Drum Worths for Different Patterns

3.2 Radial Reflector Reactivity Assessment

The radial reflector reactivity worth was assessed by a series of Monte Carlo calculations as described in Section 2. The Quantity of Interest (QOI) is the *effective* 1-group cross sections of the reflector, specifically the total cross section and scattering cross section. We parameterize the reflector reactivity in terms of the total cross section and scattering ratio. The outer reflector reactivity results are plotted in Fig. 9 and illustrated for three perspectives. The two lines correspond to the all drums out and all drums in configurations. While the drums are not included in the

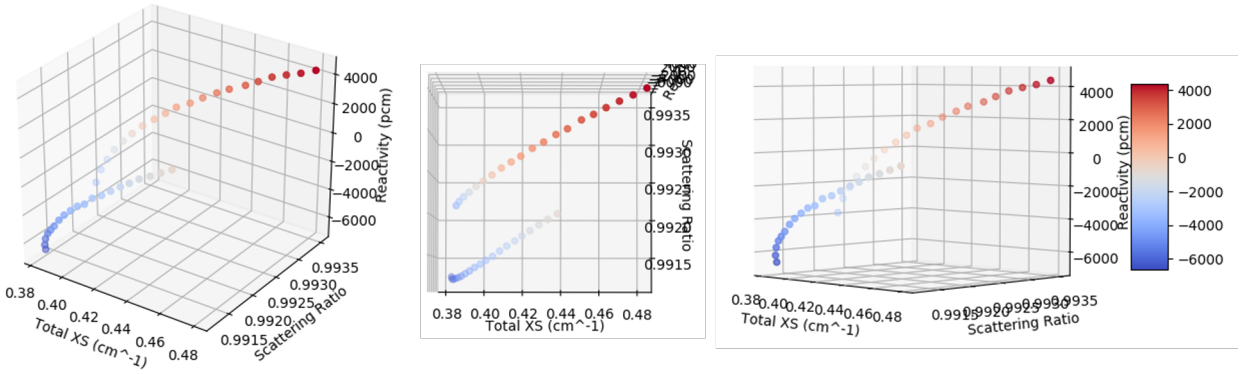

Figure 9. Outer Reflector Reactivity as a function of total cross section and scattering ratio

calculation of the 1-group cross sections, they nevertheless effect the 1-group cross section through the spectrum of the flux used to collapse the cross sections in energy. Intermediate control drum positions should fill in a smooth curve between the two lines. The line that has lower reactivity (observed as closer in the figure) is the all drums in case. Some other observations from Fig. 9 are that

- the core is under-moderated
- the scattering ratio varies little with density
- at lower densities the variation in total cross section is smaller
- at higher densities the variation in total cross section is larger
- the reflector reactivity is ~7000pcm between 10% to 200% nominal density, and about half that for 10% to 100%
- the total cross section varies by ~0.0005cm^{-1} per percent change in the moderator density; alternatively, the mean free path of neutrons in the reflector varies by ~1mm for each percent change in density when near the nominal BeO density.
- Near the nominal density the reactivity coefficient is ~44pcm per percent change in density.

From these observations we would expect there to be some small reactivity feedback from the thermal expansion of the reflector. The thermal expansion coefficient of BeO is about half that of SS304. Nominally there would be fractional percent change in the BeO density–assuming it expands unconstrained.

To help put the reflector reactivity into perspective we consider the parametric reactivity plot as a function of the control drum rotation patterns discussed previously. This is shown in Fig. 10. In Fig. 10 the control drum reactivity pattern is shown to exist as essentially a series lines. The longest line with the highest vertical slope is the all drums case. The other drum patterns are effectively shorter lines with varying slopes in the z-direction, all converging at the all drums out position. Additionally we note that the total reactivity change is similar in magnitude but larger than the reactivity envelope for a ±50% change in density of the outer reflector.

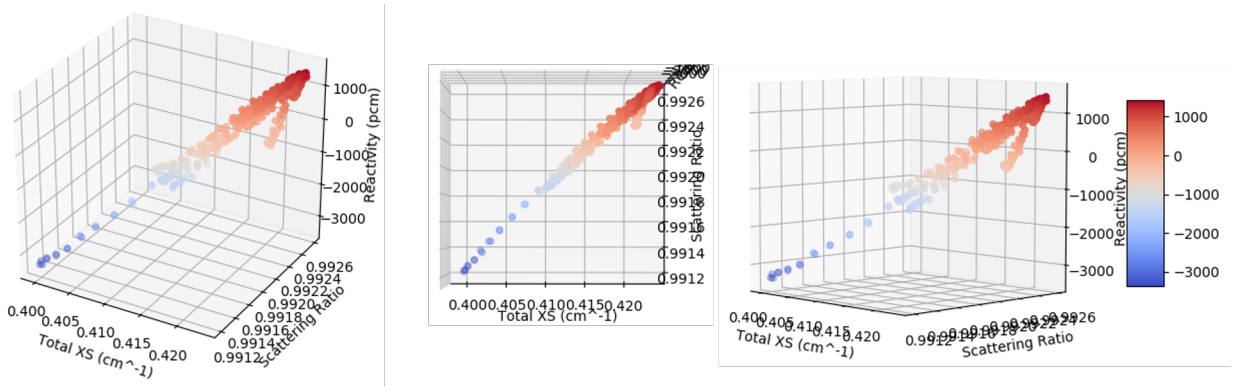

Figure 10. Control Drum Reactivity as a function of total cross section and scattering ratio

3.3 Central Reflector Reactivity Assessment

The central reflector reactivity envelope is analyzed in the same fashion as the outer reflector. The parameterized reactivity space of the central cross reflector is shown by Fig. 11. In this figure we

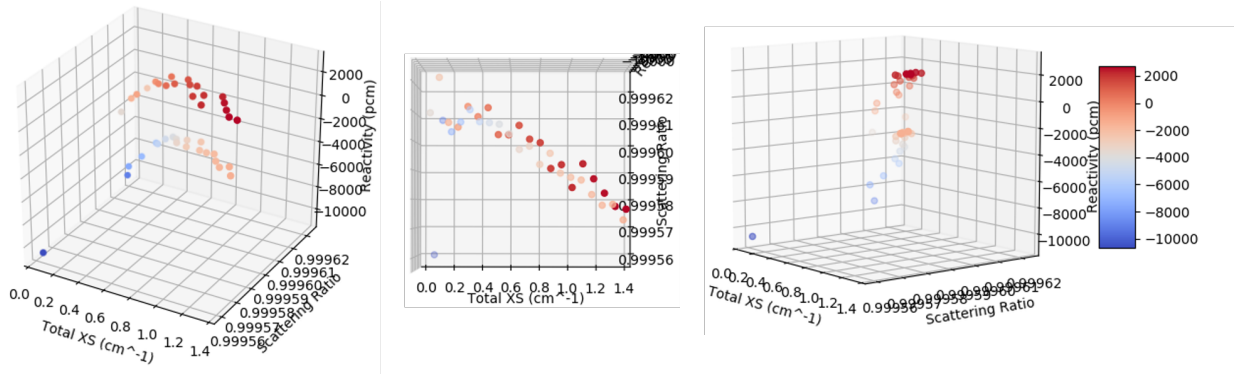

Figure 11. Central Cross Reflector Reactivity as a function of total cross section and scattering ratio

first observe there is one errant data point for which there was not sufficient time to rerun and fix. Aside from this the central reflector reactivity worth does not vary much with all drums in or out. In either case it is approximately 6,400pcm over the full range, so larger than the control drum, but less than the outer reflector. The reactivity change per percent change in density near the nominal density is ~22pcm or about half the worth of the outer reflector. As with the outer reflector there is little change in the scattering ratio. The total cross section is significantly larger than in the outer reflector, and this would be due to the high flux in the central region of the core.

3.4 Subcritical Power Module Position Reactivity Assessment

The reactivity assessment of the SPMs position was carried out using OpenMC, an open-source Monte Carlo neutron and photon transport code developed by the Computational Reactor Physics Group at the MIT [7]. OpenMC was used for this analysis rather than Serpent because the existing models for SPM separation were developed in OpenMC. The reader is reminded that in [2], both codes were shown to provide comparable results. The simulations were based on 450/50 active/inactive generations with 50,000 particles per generation, yielding uncertainties of ~20 pcm.

The integral reactivity worth was analyzed in three modes. Specifically, the position of one, two (adjacent), and all four SPMs were varied as shown in Fig. 12. The results are depicted in Fig. 13a. Here, 100% separation refers to the SPMs touching the box of the ISO container (resulting in a 21cm gap between each of the modules).

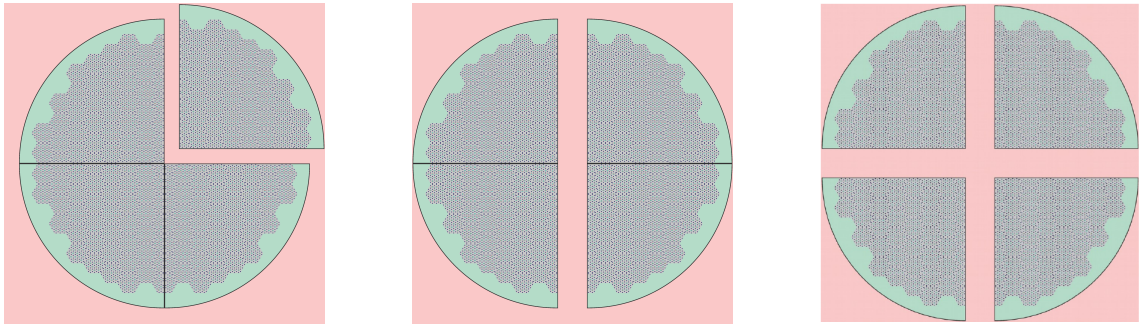

(a) 1 SPM moves **(b) 2 SPMs move** **(c) 4 SPMs move**

Figure 12. Modes of SPMs movement

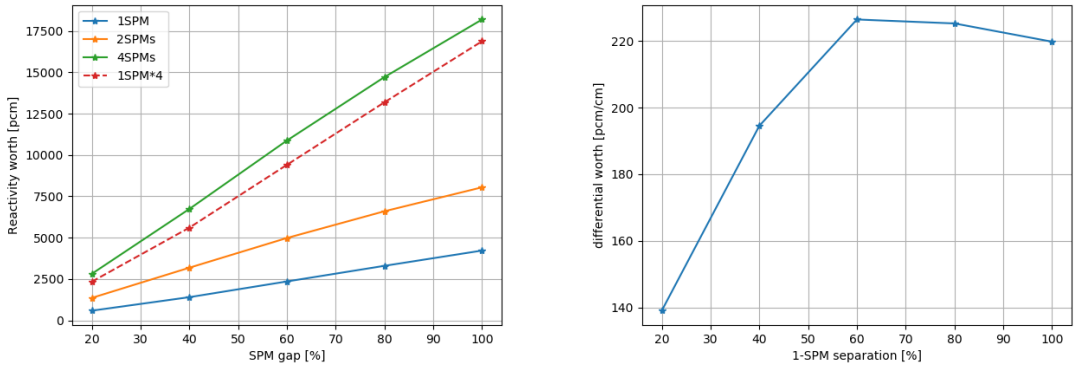

(a) Integral worth **(b) Differential worth**

Figure 13. Integral and differential reactivity worth of SPM position

It is seen that the qualitative behavior of the reactivity for all modes is similar. However, while the total worth of 2 SPMs is about twice the worth of 1 SPM, that is not the case with 4 SPMs, which has a higher worth-per-SPM value. To demonstrate this, the integral curve of 1 SPM worth multiplied by 4 is depicted, showing smaller values of ~15% compared to the 4 SPMs case.

To analyze the linearity of the worth curve, the differential worth of 1 SPM position is depicted in Fig. 13b. The differential curve is found to be non-monotonous. The worth has a minimal value of 140 pcm/cm when SPM separation is small, but as the separation increses this value also increases, until it reaches a maximum of ~230 pcm/cm at 60% separation. From this point the worth decreases slowly until it reaches 220 pcm/cm at 100% separation.

We conclude that for separation values in the range 0-60%, the differential worth strongly depends on the position. Although the Holos design no longer uses movable SPMs, should future reactor concepts based on varying the geometric configuration to maintain criticality be pursued, the

information gained from this analysis should be valuable in providing some intuition as to the system reactivity perturbations. This value is inherent due to the fact that this dependence must ultimately be considered in the design of a control system based on position.

4. CONCLUSIONS AND FUTURE WORK

4.1 Conclusions

The variable reflector reactivity envelope was explored generally through assumed changes in the reflector material density as a simple way to adjust its moderating power. This revealed that either the central or outer reflector have sufficient contributions to reactivity that control devices may be developed yet. What is still not clear at this point is what types of passive mechanisms may be employed to get an ideal reactivity response suitable for load follow. The notion of a variable reflector is further analyzed through rotation of the control drums. Analysis of the control drums shows that these are more than sufficient for reactivity control during load follow based on the preliminary work documented in [8]. Lastly, the reactivity worth curves of the SPM separation were determined. For variations to the reflector (outer or central) by adjusting the moderating power, changing the SPM spacing, or rotating the control drums in various patterns, all approaches were demonstrated to contain sufficient reactivity to provide reactivity control. We explicitly define a "sufficient" amount of reactivity control as demonstrating subcritical and supercritical multiplication factors.

Analytic models for the integral drum worth, Eq. (11), and differential drum worth, Eq. (13), were developed from first order perturbation theory. These models were shown to be reasonably accurate for a wide range of control drum positions. Limitations and systematic errors of the analytic drum worth models were also identified.

4.2 Future Work

In future work related to the analyses presented here we will:

- make further refinements for consistency to the Monte Carlo models
- rerun the models with improved statistics
- explore corrections to Eqs. (11) and (13) to better capture all rod patterns
- extend the analysis here as a function of burnup

Furthermore, we will consider:

- parameterizing the data in a different way
- developing a more quantitative discussion of some of the results here
- new concepts for variable reflectors that allow for a passive response.

Additional future work that will make use of the results here will be the comparisons to the local temperature reactivity responses. This will be fully documented with updated results here in the next project milestone.

Furthermore, after the year 1 milestone, the work will start to focus more on the development and analysis of the automated control of the control drums for flexible power operation. This is the focus of the upcoming milestone due 12/31/2020. Preliminary results on this task documented here [8] use a constant reactivity coefficient for the drums, which is not realistic. This analysis will continue with the development of an explicit comparison of representative control drum reactivity worth curves to a constant value (as was done here for the SPMs). In the development and analysis of the control algorithms, we may further use these to identify reactivity worth curves that optimize control.

REFERENCES

[1] V. Seker and B. Kochunas. "Assessment of Local Temperature Reactivity Response in Multi-Module HTGR Special Purpose Reactor." Technical report, University of Michigan, Ann Arbor (2020).

[2] T. Stauff, N. and Lee, C. and Shriwise, P. and Miao, Y. and Hu, R. and Vegendla, P. and Fei. "Neutronic Design and Analysis of the Holos-Quad Concept." Technical report, Argone National Laboratory (2019).

[3] "ARPA-E | Transportable Modular Reactor." URL `https://arpa-e.energy.gov/?q=slick-sheet-project/transportable-modular-reactor`.

[4] N. Stauff. "Design Specifications of the Holos-Quad." private communication (2020).

[5] J. Leppänen, M. Pusa, T. Viitanen, V. Valtavirta, and T. Kaltiaisenaho. "The Serpent Monte Carlo code: Status, development and applications in 2013." *Annals of Nuclear Energy*, **volume 82**, pp. 142–150 (2015).

[6] J. Lee. *Nuclear Reactor Physics and Engineering*. John Wiley & Sons, Inc, Hoboken, NJ, USA (2019).

[7] P. K. Romano, N. E. Horelik, B. R. Herman, A. G. Nelson, B. Forget, and K. Smith. "OpenMC: A state-of-the-art Monte Carlo code for research and development." In *SNA+ MC 2013-Joint International Conference on Supercomputing in Nuclear Applications+ Monte Carlo*, pp. 6–16 (2014).

[8] S. Choi, S. Kinast, V. Seker, C. Filippone, and B. Kochunas. "Preliminary Study of Model Predictive Control for Load Follow Operation of Holos Reactor." *Transactions of the American Nuclear Society*, **volume 122**, pp. 660–663 (2020). URL `https://dx.doi.org/10.13182/T122-32327`.